# Real time quantum correlation functions. I. Centroid molecular dynamics of anharmonic systems

Goran Krilov and B. J. Berne
*Department of Chemistry, Columbia University, 3000 Broadway, New York, New York 10027*

(Received 28 July 1999; accepted 1 September 1999)

We investigate the accuracy of the recently proposed centroid molecular dynamics (CMD) method [J. Cao and G. A. Voth, J. Chem. Phys. **100**, 5106 (1994)] in the presence of highly anharmonic steep short range repulsive potentials. Such potentials are often present in condensed phases and govern collisions between solvent particles. We compare the results of CMD simulations with exact quantum results for several model one- and two-dimensional nondissipative systems and a one-dimensional system under isobaric conditions. We show that, for nondissipative systems, CMD is accurate only for very short times, and is unable to reproduce the effects of quantum coherences, which play an important role in these few-dimensional systems. CMD gives much better results under isobaric conditions. The correlation functions and the general lineshape of the absorption cross-section in the dipole limit are well reproduced. This is primarily due to dephasing of quantum coherences through inhomogeneous broadening. © *1999 American Institute of Physics.* [S0021-9606(99)51644-9]

## I. INTRODUCTION

Accurate treatment of quantum effects in many body condensed phase systems is perhaps one of the most challenging tasks of quantum statistical mechanics. Due to the great complexity of these systems, standard methods based on basis set expansions and wave-packet propagations are not feasible, even for systems consisting of relatively few particles.

The advent of techniques based on the Feynman path integral formulation of statistical mechanics[1] made it possible to extend simulation methods such as Monte Carlo (MC) and molecular dynamics (MD) to the quantum domain. In such a formulation, the computation of the quantum partition function involves the evaluation of an imaginary or Euclidean time path integral:

$$Q=\mathrm{Tr}\,\rho=\int dq\int_q^q Dq(\tau)\exp\left[\frac{-S[q(\tau)]}{\hbar}\right], \tag{1}$$

where $S[q(\tau)]$ is the Euclidean time action functional

$$S[q(\tau)]=\int_0^{\beta\hbar} d\tau\, H(q(\tau)). \tag{2}$$

For computational purposes, it is necessary to discretize the path integral, with primitive or Trotter discretization[2] being the most common. In this approximation, the Euclidean time is split into increments $\epsilon=\beta\hbar/P$ which leads to the following expression for the partition function

$$Q_P=\left(\frac{mP}{2\pi\hbar^2\beta}\right)^{P/2}\int dq_1\ldots dq_P\, e^{-\beta\Phi_P(\mathbf{q})}, \tag{3}$$

with the condition $q_t=q(t\beta\hbar/P)$ and $q_{P+1}=q_1$, where

$$\Phi_P(\mathbf{q})=\sum_{t=1}^{P}\left[\frac{mP}{2\hbar^2\beta^2}(q_t-q_{t+1})^2+\frac{V(q_t)}{P}\right], \tag{4}$$

which converges to the exact result as[2] $P\to\infty$. The above system is isomorphic to a classical system with the potential $\Phi_P$. Path integral Monte Carlo (PIMC)[3] and path integral molecular dynamics (PIMD)[4] simulations, developed to compute the integral in Eq. (3) have been very successful in calculating equilibrium properties of complex quantum systems. However, many important properties of such systems, in particular many of those probed experimentally, are time-dependent. These include transport coefficients, light and neutron scattering cross-sections, dipole relaxation times, and reaction rates.

A novel and very promising method for approximate computation of real-time quantum position and velocity correlation functions, called centroid molecular dynamics (CMD) has recently been introduced by Cao and Voth.[5–8] This method has been used to calculate dynamic properties such as absorption cross-sections in the dipole limit and diffusion coefficients. It has so far been applied to systems such as water,[9] proton solvated in water,[10,11] lithium-para hydrogen clusters,[12] and slabs,[13] and more recently, liquid para-hydrogen[14] and liquid helium.[15]

One of the main impediments to the wider application of CMD has been the insufficient understanding of the limitations of the method. Due to this fact, it has been difficult to establish well-defined regions of applicability. This poses a significant problem, particularly since CMD was developed primarily to treat many-body condensed systems, for which there are no exact quantum results available for comparison. Studies done so far on such systems have relied primarily on comparison with experimental results to estimate the accuracy of the method. This is inadequate to characterize the

 

accuracy of the dynamics, since model potentials used in these calculations often fail to represent all the effects of physical potentials which are the ones that are probed experimentally. Therefore, in order to truly evaluate CMD as an approximation to the dynamics of the system, one has to consider systems for which it is possible to obtain numerically exact dynamical quantities.

It is known that the error in correlation functions calculated through CMD grows as the potential becomes more anharmonic.[7] On the other hand, potentials encountered in the condensed phase often contain highly anharmonic interactions such as very steep short range repulsive interactions between solvent molecules. In this article we address the question of the accuracy of CMD in the presence of such interactions. In general, we find that CMD gives very good results for short times in all cases studied, particularly for the systems in which the quantum coherences are dampened through dephasing. This served as a motivation for using short time CMD data in conjunction with imaginary time data in maximum entropy numerical analytic continuation method of the accompanying following article.[16]

In Sec. II we present the CMD method and the particular form of implementation. In Sec. III we evaluate the accuracy of CMD for several nondissipative model systems and for an exactly solvable inhomogeneously dephasing system. We conclude in Sec. IV.

## II. CMD METHOD AND IMPLEMENTATION

The fundamental quantity in the formulation of CMD is the path centroid variable[1] $q_0$, which is the imaginary time average of a closed Feynman path

$$q_0=\frac{1}{\beta\hbar}\int_0^{\beta\hbar} d\tau\, q(\tau). \tag{5}$$

In the discretized picture this is simply the center-of-mass of the isomorphic polymer chain of quasiparticles. One can define the centroid density,[17] $\rho_c(q_c)$, as the sum over all closed paths with centroids at $q_c$,

$$\rho_c(q_c)=\int Dq(\tau)\,\delta(q_c-q_0)\exp\left[\frac{-S[q(\tau)]}{\hbar}\right]. \tag{6}$$

Similarly, the canonical partition function, and relevant ensemble averages can likewise be expressed as integrals of the centroid density over all possible positions of the centroid,

$$Q=\int dq_c\ \rho_c(q_c). \tag{7}$$

Cao and Voth developed an approximate method for calculating the real-time position and velocity correlation functions of a quantum system based on the path centroid variable.[6] The CMD method is based on classical time evolution of the centroid variable on the potential surface defined by the excess quantum free energy of the centroid,

$$V_c(q_c)=-k_bT\ln\left[\frac{\rho_c}{\sqrt{m/2\pi\hbar^2\beta}}\right]. \tag{8}$$

The classical equation of motion for the centroid variable is then given by

$$m\ddot{q}_c(t)=F_c, \tag{9}$$

where $F_c=-dV_c/dq_c$ is the centroid force

$$F_c(q_c)=-\frac{1}{\rho_c}\int Dq(\tau)\,\delta(q_c-q_0)\frac{dV(q)}{dq}\times\exp\left[\frac{-S[q(\tau)]}{\hbar}\right]. \tag{10}$$

By integrating the equations of motion, one can obtain the centroid trajectory $q_c(t)$, which in turn can be used to compute the centroid position correlation function

$$C_c(t)=\langle q_c(t)q_c(0)\rangle_{\rho_c}, \tag{11}$$

where $\langle\ldots\rangle_{\rho_c}$ now signifies the average over the initial conditions given by the phase space centroid density. It has been shown[7,18] that the centroid position correlation function $C_c(t)$ is an approximation to the Kubo transformed position correlation function[19]

$$\psi(t)=\frac{1}{\beta}\int_0^{\beta} d\lambda\langle q(t+i\lambda\hbar)q(0)\rangle, \tag{12}$$

which in turn is related to the real-time quantum position correlation function $C(t)$ by

$$I(\omega)=\frac{\beta\hbar\omega}{2}\left[\coth\left(\frac{\beta\hbar\omega}{2}\right)+1\right]\tilde{\psi}(\omega). \tag{13}$$

Here $\tilde{\psi}(\omega)$ is the Fourier transform of $\psi(t)$ and $I(\omega)$ is the spectral density given by

$$I(\omega)=\int_{-\infty}^{\infty} dt e^{+i\omega t}C(t). \tag{14}$$

For quadratic potentials $C_c(t)$ is exactly equal to the Kubo transformed position correlation function. In other cases one can recover the approximate real-time position correlation function through an inverse transform of $I(\omega)$. In addition to the correlation function, the above relationship can be used to compute the quantum photon absorption cross-section, $\sigma(\omega)$, in the dipole limit[20]

$$\sigma(\omega)=\frac{4\pi\omega}{\hbar c}(1-e^{-\beta\hbar\omega})I(\omega). \tag{15}$$

The most demanding aspect of the CMD method is the computation of the centroid force, that is the evaluation of the path integral in Eq. (10). In principle, this can be done using any conventional method for imaginary-time path integrals with inclusion of the centroid constraint. However, since the centroid force needs to be recalculated at every time step, direct evaluation of Eq. (10) through PIMC or PIMD is computationally very demanding, even for systems with relatively few degrees of freedom. Several approximate approaches for obtaining the centroid force based on pseudopotentials[21] or the effective harmonic method[8] have been used. These, although computationally less demanding, introduce errors in the centroid force and hence were not used in present work. Instead we use two algorithms, both

based on the direct evaluation of the centroid force. In all cases, primitive discretization is used to approximate Eq. (10) by

$$F_c(q_c(t)) = \left(\frac{mP}{2\pi\hbar^2\beta}\right)^{P/2} \int dq_1 \cdots dq_P \; \delta\left(q_c - \frac{1}{P}\sum_{t=1}^{P} q_t\right) \times \left(\frac{1}{P}\sum_{t=1}^{P} \left.\frac{dV(q)}{dq}\right|_{q=q_t}\right) e^{-\beta\Phi_P(\mathbf{q})}, \tag{16}$$

where $\Phi_P(\mathbf{q})$ is given in Eq. (4).

In the first implementation, henceforth referred to as the ''grid'' method, we compute the centroid force in advance on a grid of points and store the values. The force at each grid point is obtained by performing a staging PIMC[22] simulation, while keeping the centroid constrained to a given grid point. Sufficient number of configurations were sampled to obtain a converged value of the force at each grid point. The CMD trajectories were then generated via the standard Verlet algorithm, the centroid force at each time step being computed from the grid values through linear interpolation. This method is feasible only for systems with few degrees of freedom, and can be computationally demanding even for those, particularly in the cases of sharply varying potentials, which require dense grids. On the other hand, once the force grid has been computed, one can evaluate a large number of CMD trajectories with a small computational effort, thereby allowing better statistical sampling of initial conditions which leads to less noisy results.

The second implementation of the CMD method is based on what Cao and Voth refer to as ''on-the-fly'' algorithm.[8] With this approach the centroid force is calculated at each time step, with the path integral averaging being performed concurrently along with the dynamic evolution of the centroid trajectory. Each CMD time step $\Delta t$ is divided into $N$ small steps $\delta t$. At each small time step the following is performed:

(i) A MC configuration is generated by performing a staging PIMC move.
(ii) The positions of all the beads are shifted uniformly to preserve the position of the centroid.
(iii) The centroid constrained configuration is accepted or rejected according to the Metropolis criterion.
(iv) The centroid force is averaged over $n$ such configurations and the centroid is then propagated for the step $\delta t$ using the standard Verlet algorithm.

By repeating the above procedure for $N$ small time steps, one completes a single time step $\Delta t$ of the CMD trajectory integration. Note that through this algorithm one effectively averages the centroid force over $N_{\mathrm{MC}} = n \times N$ MC passes, but the dynamic averaging is numerically more efficient and generally leads to smoother trajectories, as opposed to averaging the force for $N_{\mathrm{MC}}$ passes and then propagating for the full time step $\Delta t$.

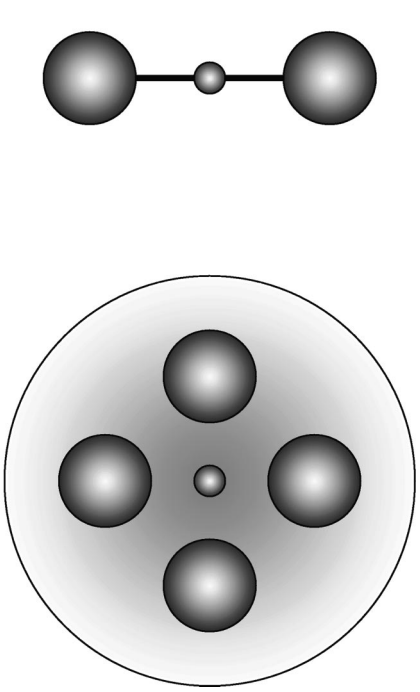


FIG. 1. A diagrammatic representation of the anharmonic potentials studied, for the (a) one-dimensional and (b) two-dimensional cases. The small circle represents the quantum particle. The large circles show the positions of the fixed soft spheres. The shading in (b) denotes the presence of the harmonic binding potential.

## III. RESULTS OF CMD SIMULATIONS FOR TEST SYSTEMS

### A. One-dimensional box with soft walls

We consider a one-dimensional system of a quantum particle trapped between two soft spheres, the centers of which are fixed at $-a$ and $a$ and the interaction given by

$$V(q) = \frac{1}{|q-a|^{12}} + \frac{1}{|q+a|^{12}}. \tag{17}$$

The system is depicted diagrammatically in Fig. 1(a).

The phase space distribution of centroid initial positions $q_c$ was obtained through staging PIMC,[22] while the centroid momenta $p_c$ were sampled from a Gaussian distribution. The number of Trotter slices was set to $P=128$ for the higher temperature and $P=256$ for the lower one. A total of $10^5$ initial conditions were generated from $10^6$ MC passes for each temperature.

The ''grid'' method was employed to compute the centroid force using the centroid-constrained staging PIMC at 1000 grid points, equally spaced between $-a$ and $a$. A total of $5\times10^4$ MC passes were used for each grid point. Linear interpolation was used to obtain the force during CMD simulations. The value of $a$ was set to 2.5 a.u., which is typical of the spacing between liquid molecules at normal conditions. The mass of the particle was set to 1.0 a.u. and the CMD trajectories were computed for each set of initial conditions. The approximate real-time position correlation functions were then computed as described in Sec. II, by averaging over $10^5$ trajectories.

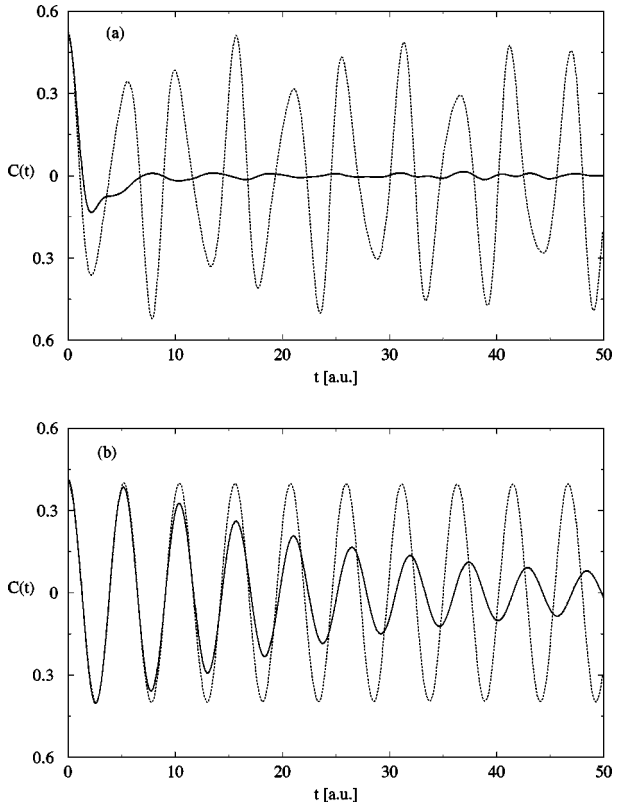


FIG. 2. The real part of the quantum position correlation function for a particle interacting with a 1D soft sphere potential. The dotted line is the exact quantum result and the solid line is the CMD approximation. The results are shown for two values of the inverse temperature $\beta=1/k_bT$: (a) $\beta=1.0$ a.u. and (b) $\beta=10.0$ a.u.

The exact quantum position correlation functions were computed from the eigenstates according to

$$\langle q(t)q(0)\rangle=\frac{1}{Q}\sum_m\sum_n e^{-\beta E_n-(it/\hbar)(E_m-En)}|\langle m|q|n\rangle|^2. \tag{18}$$

A total of 100 lowest-lying states were used in the above computation. The eigenstates were computed on an $N\times N$ grid with $N=500$ by diagonalizing the grid representation of the Hamiltonian generated through the B-spline method.[23] In Fig. 2(a) we show the real part of the position correlation function obtained from CMD through Eq. (13) along with the exact result for $\beta=1.0$ a.u. where $\beta$ is the inverse temperature $\beta=1/k_BT$. Figure 2(b) gives the same results for a lower temperature $\beta=10.0$ a.u.

Comparing with the exact quantum results, one can see that in both cases CMD accurately reproduces the dynamics only for very short times in this strongly anharmonic regime. Interestingly, the results are better for the lower temperature case which is more strongly quantum in nature. Such behavior was also observed by Jang and Voth.[24] This is primarily due to the fact that at such low temperature, the system is ground state dominated, with only the ground state and the first excited states determining the dynamics. Since in this case we effectively have a two-state system specified by a single frequency $\omega=(E_1-E_0)/\hbar$, the nearly harmonic behavior of the exact quantum result seen in Fig. 2(b) reflects these quasiharmonic oscillations. Since CMD is exact for harmonic cases, the method is able to better capture these harmonic-like oscillations. However, to generalize this reasoning, one would have to show that the curvature of the centroid potential at low temperature approaches the value $[(E_1-E_0)/\hbar]^2$, where $E_0$ and $E_1$ are the energies of the ground state and the first excited state of the exact potential. Recent studies by Ramirez *et al.* on the centroid potential in the zero temperature limit support this idea.[25,26] In the case of an intermediate temperature, there are several excited states that are populated appreciably and thereby contribute to the dynamics. As a result, the anharmonicity is more pronounced, while still retaining a strong quantum character, and CMD fails to reproduce the exact results.

In both cases though, CMD results eventually deviate from the exact ones, as CMD is unable to capture the quasiperiodic behavior of correlation functions resulting from quantum coherence effects. This is not surprising, since the coherence information is lost in the averaging process used to calculate the centroid force, which has an effect of ''smearing out'' these features. It is important to note, however, that for the systems in which coherent effects play an important role, CMD cannot be expected to perform acceptably and a different method should be used, if reliable long-time dynamic information is required.

### B. Two-dimensional soft sphere potential

The strong coherence effects and intrinsic quasiperiodicity are inherent artifacts of the symmetric one-dimensional potential studied above. In a real, multiparticle system such coherences would certainly be diminished, if not eliminated completely through dephasing effects resulting from chaotic collisions between system particles and interactions with a dissipative environment. In order to eliminate these 1D artifacts, we next consider a quantum particle interacting with a two-dimensional potential, consisting of four soft spheres of unit radius located at $(\pm\sqrt{2}a,0)$ and $(0,\pm\sqrt{2}a)$. The potential has the form

$$V(x,y)=\frac{1}{|x-\sqrt{2}a|^{12}}+\frac{1}{|x+\sqrt{2}a|^{12}}+\frac{1}{|y-\sqrt{2}a|^{12}}+\frac{1}{|y+\sqrt{2}a|^{12}}+\frac{1}{2}m\omega_0^2(x^2+y^2), \tag{19}$$

where the last term is a weak harmonic interaction included to keep the system bound. A diagrammatic representation of the system is given in Fig. 1(b). One should note that classical dynamics for this two-dimensional system would likely be chaotic, since the strong repulsions should lead to a behavior similar to a Sinai billiard.

The eigenstates used to calculate the exact time correlation functions were obtained from a grid-based filter-diagonalization method with singular value decomposition.[27,28] A total of 100 lowest-lying states were used in calculations. The centroid force was evaluated on a $50\times50$ grid using the ''grid method.'' A total of $5\times10^4$ MC passes were used for each grid point. Two-dimensional linear interpolation was used to obtain the force during CMD simu-

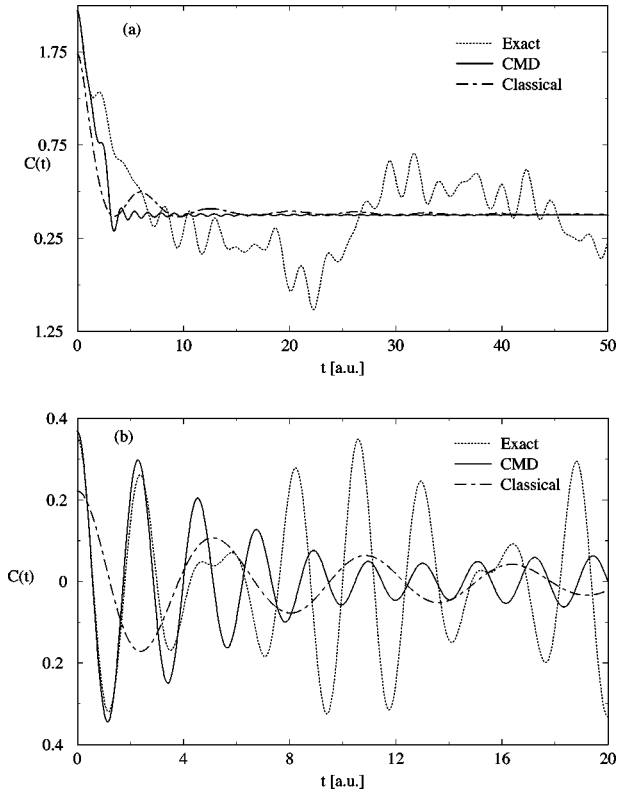


FIG. 3. Real part of the quantum position correlation function for a particle interacting with a 2D potential consisting of four symmetrically placed soft spheres. The dotted line is the exact quantum result obtained through filter diagonalization and the solid line is the CMD approximation. The results are shown for two values of the inverse temperature $\beta=1/k_bT$: (a) $\beta=1.0$ a.u. and (b) $\beta=5.0$ a.u. The dot-dashed line is the classical correlation function for the corresponding temperatures.

lations. The value of $a$ was set to 2.5 a.u. and the harmonic frequency and the mass of the particle $\omega_0=m=1.0$ a.u. The CMD simulations were performed at two different inverse temperatures of $\beta=1.0$ a.u. and $\beta=5.0$ a.u. The real parts of the position correlation functions for the two cases are shown compared to the exact results in Fig. 3(a) and 3(b).

As can be seen the exact results still maintain a quasiperiodic behavior which is a consequence of quantum recurrences. CMD results, on the other hand, show an even faster dephasing behavior than in the one-dimensional case. This can be explained by the fact that the CMD trajectories loose their periodicity faster through multiple collisions with convex surfaces of the soft spheres. One should note, though, that the 2D system analyzed does not suffer from the artifacts present in the 1D case and that a large number of quantum states contribute significantly to the dynamics. Yet the dephasing is still slow and quantum coherences play an important role even at short times. It is therefore plausible that such coherences might play an important role in larger systems as well.

The fact that CMD captures the short-time behavior reasonably well suggests that for a dissipative system, in which the quantum coherences are dephased through the interaction with the dissipative environment, CMD might give fairly accurate results, even for strongly anharmonic potentials. However, the only dissipative systems for which the exact quantum results are available involve quadratic potentials. Since CMD is exact for such potentials, they do not offer a good test for the method. We will instead consider a case of inhomogeneous pressure broadening.

### C. Isobaric one-dimensional box with soft walls

We next consider one-dimensional analog of the 2D soft sphere potential described in the previous section, given by

$$V(q)=\frac{1}{|q-a|^{12}}+\frac{1}{|q+a|^{12}}+\frac{1}{2}\,m\omega_0^2q^2. \tag{20}$$

The weak harmonic potential is retained to insure a sufficient separation of the eigenstates at large values of $a$, and allow the computation of the exact quantum results using a finite number of states. The inhomogeneous line broadening is accomplished by imposing a constant pressure $P$ on the system, which leads to the normalized distribution of $a$ given by

$$\mathcal{P}(a)da=\frac{1}{\Delta}\,e^{-2\beta Pa}Q(\beta,a)da. \tag{21}$$

The centroid position correlation function can then be reformulated in the isobaric ensemble

$$C_c^P(t)=\frac{1}{\Delta}\int_0^\infty da\; e^{-2\beta Pa}Q(\beta,a)\langle q_c(t)q_c(0)\rangle_{\rho_c}, \tag{22}$$

where $Q(\beta,a)$ is the canonical partition function for a particular $a$, and $\Delta$ is the isobaric partition function. With these results, one can obtain the approximation to the spectral density and the absorption cross-section via Eqs. (14) and (15). We performed CMD simulations for two values of the external pressure, $P=0.33$ a.u. and $P=1.0$ a.u., both at the inverse temperature $\beta=5.0$ a.u. The harmonic frequency $\omega_0$ is chosen to be unity in both cases. The initial centroid positions and momenta were sampled as in Sec. II, whereas the volumes $2a$ were sampled by MC from $P(a)$. A total of $10^4$ centroid trajectories were generated for each pressure using the ''on-the-fly'' method[8] in which the centroid force is calculated dynamically along with the time-evolution of the centroid.

The exact quantum position correlation functions were computed in the following fashion. We construct a matrix representation of the Hamiltonian on a uniform grid using the B-spline method.[23] The Hamiltonian is then diagonalized and the resulting eigenstates used to compute both the position correlation function $\langle q(t)q(0)\rangle_a$ and the partition functions $Q(\beta,a)$. The final result is obtained by integrating the correlation functions over $P(a)$

$$C(t)=\frac{1}{\Delta}\int_0^\infty da\; e^{-2\beta Pa}Q(\beta,a)\langle q(t)q(0)\rangle_a. \tag{23}$$

We used 20 lowest-lying states and a total of 1000 uniformly spaced values of $a$ to insure convergence of the quantum results. In Fig. 4 we show the real part of the quantum position autocorrelation function computed by CMD compared to the exact result for $P=0.33$ a.u. and $P=1.0$ a.u. Both cases show rather fast dephasing of quantum coherences, and the agreement between the exact quantum and CMD results

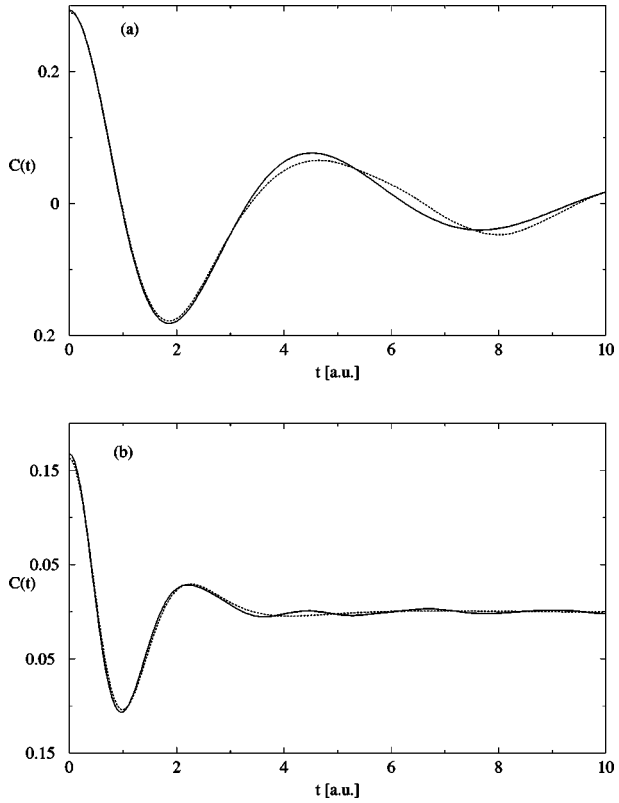


FIG. 4. Real part of the quantum position correlation function for a particle in a constant pressure 1D soft sphere potential with a weak harmonic component. The dotted line is the exact quantum result and the solid line is the CMD approximation. The results are shown for two values of the external pressure $P$: (a) $P=0.33$ a.u. and (b) $P=1.00$ a.u. Both systems were studied at the inverse temperature $\beta=5.0$ a.u.

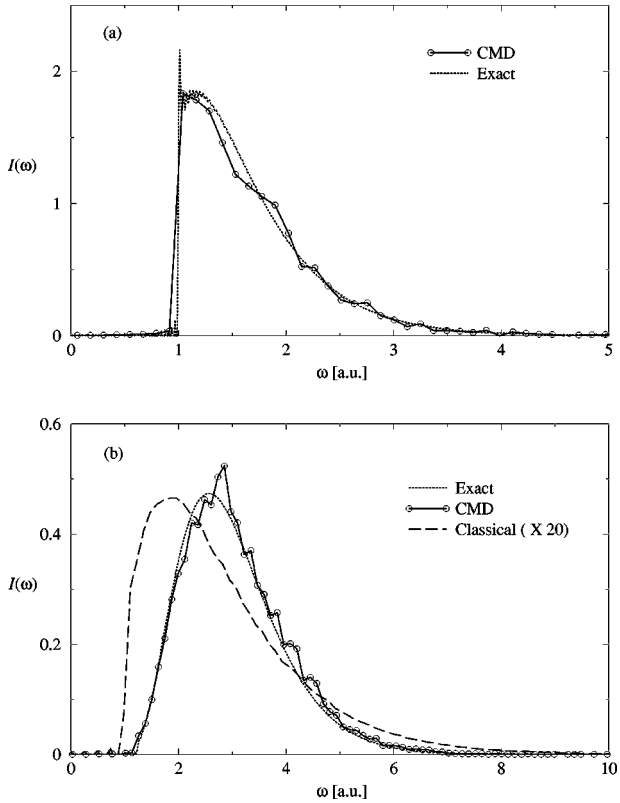


FIG. 5. The spectral density for a particle in a constant pressure 1D soft sphere potential with a weak harmonic component. The dotted line shows the exact quantum result and the solid line with open circles the CMD result. The results are shown for two values of the external pressure $P$: (a) $P=0.33$ a.u. and (b) $P=1.00$ a.u. Both were computed by a direct Fourier transform from the correlation functions in Fig. 4. The dashed line in (b) is the corresponding classical spectrum, magnified 20 times.

is excellent, particularly in the higher pressure case. As a more stringent test of the accuracy with which CMD reproduces quantum dynamics, we computed the spectral density $I(\omega)$ from the correlation function by a direct Fourier transform in Eq. (14). The results for the two pressures are shown in Fig. 5. No attempt was made to window the data to avoid introducing artificial broadening. The CMD spectra were coarse-grained following the Fourier transform to remove some of the noise resulting from the finite time cutoff. For the higher pressure case, we also computed the classical spectral density, which is shown in Fig. 5(b) with a magnification of 20 times. The large difference in intensity as well as in lineshape and peak position between the classical and quantum spectra demonstrates the dominance of quantum effects in the studied system.

The principal spectral feature is the transition from the ground state to the first excited state which is manifested as a broad peak in both figures. The inhomogeneous broadening is due to the isobaric distribution of the volumes $a$. The sharp peak at $\omega=1.0$, observable in the low pressure case, is due to the harmonic $|0\rangle \rightarrow |1\rangle$ transition which becomes dominant at large volumes, as it represents the lower bound on the energy level spacing and hence the lowest observable frequency. The high pressure case does not show this feature since the spectrum is shifted to higher frequencies and the absorption at $\omega=\omega_0$ is negligible.

One can observe that the CMD spectrum captures most of features of the exact quantum spectrum for both pressures, the agreement being somewhat better for the higher pressure case. Most notably, the high frequency tail is accurately reproduced as well as the general lineshape, including the height and the width of the peak. The accuracy is poorer at lower frequencies, consistent with the fact that CMD gives accurate short-time dynamics which determines the high frequency contributions, while the error increases at longer times.

The fact that CMD is able to reproduce quantum dynamics with high accuracy for a highly anharmonic dephasing is very encouraging. In particular the results show that short-time dynamic information is consistently captured with high accuracy in all cases studied. In the accompanying article[16] we show how one can use this short-time information in conjunction with imaginary-time dynamics to extract accurate results for equilibrium dynamics of quantum systems.

## IV. CONCLUSION

In this article we have investigated the merits and limitations of centroid molecular dynamics as a method of approximating equilibrium quantum dynamics in condensed phase systems. In particular, we evaluated the accuracy of CMD for treating systems which interact through highly anharmonic potentials, such as the $1/r^{12}$ soft sphere repulsion.

Such interactions govern molecular collisions and often play an important role in the dynamics of liquids. Our findings show that, for one- and two-dimensional anharmonic systems, in which short-time quantum coherences are dominant, CMD trajectories dephase too quickly and are unable to capture these coherences. The short-time dynamics is, however, accurately reproduced.

It should be noted that for coherent anharmonic systems CMD gives notably better results for low temperatures. At a glance, this result is opposed to the general notion that the accuracy of CMD should improve as one goes to higher temperatures and approaches the classical limit. The reason for such behavior is that low temperatures are ground state dominated, and the dynamics is determined solely by the ground state and the first excited state. This leads to harmonic-like coherent behavior that is captured by CMD, since at low temperatures the centroid dynamics is dominated by quasiharmonic oscillations with an effective frequency determined by the curvature of the centroid potential at its minimum. Recently it was shown that in the zero temperature limit this effective frequency is related to the splitting between the ground state and the first excited state.[25,26] On the other hand, in the intermediate temperature range, where several excited states contribute to the dynamics, the anharmonicity if the potential is more pronounced, and CMD is unable to account for the coherent behavior.

We find that for systems which exhibit strong dephasing, such as the inhomogeneously broadened versions of the soft sphere repulsion, CMD gives remarkably accurate results, in spite of the high anharmonicity of the potential. Based on this, we conclude that CMD is likely to give an acceptable approximation especially at short times to quantum dynamics in those cases where quantum coherences are negligible. We use the observed accuracy of the centroid molecular dynamics method at short times for highly anharmonic system as a justification for the use of short-time CMD data in the numerical analytic continuation method of the accompanying article.[16]

## ACKNOWLEDGMENTS

This work was supported by a grant from the National Science Foundation. We would like to thank Dr. Eran Rabani for many useful discussions and Marc Pavese for helpful comments on the CMD method.

[1] R. P. Feynman and A. Hibbs, *Quantum Mechanics and Path Integrals* (McGraw-Hill, New York, 1965).
[2] M. F. Trotter, Proc. Am. Math. Soc. **10**, 545 (1959).
[3] H. F. Jordon, Phys. Rev. **171**, 128 (1968).
[4] M. Parinello and A. Rahman, J. Chem. Phys. **80**, 860 (1984).
[5] J. Cao and G. A. Voth, J. Chem. Phys. **100**, 5093 (1994).
[6] J. Cao and G. A. Voth, J. Chem. Phys. **100**, 5106 (1994).
[7] J. Cao and G. A. Voth, J. Chem. Phys. **101**, 6157 (1994).
[8] J. Cao and G. A. Voth, J. Chem. Phys. **101**, 6168 (1994).
[9] J. Lobaugh and G. A. Voth, J. Chem. Phys. **106**, 2400 (1997).
[10] J. Lobaugh and G. A. Voth, J. Chem. Phys. **104**, 2056 (1996).
[11] M. Pavese, S. Chawla, D. Lu, J. Lobaugh, and G. A. Voth, J. Chem. Phys. **107**, 7428 (1997).
[12] K. Kinugawa, P. B. Moore, and M. L. Klein, J. Chem. Phys. **106**, 1154 (1997).
[13] K. Kinugawa, P. B. Moore, and M. L. Klein, J. Chem. Phys. **109**, 610 (1998).
[14] K. Kinugawa, Chem. Phys. Lett. **292**, 454 (1998).
[15] S. Miura, S. Okazaki, and K. Kinugawa, J. Chem. Phys. **110**, 4523 (1999).
[16] G. Krilov and B. J. Berne, J. Chem. Phys. **111**, 9147 (1999), following paper.
[17] R. P. Feynman, *Statistical Mechanics* (Addison-Wesley, Reading, MA, 1998).
[18] S. Jang and G. A. Voth, J. Chem. Phys. **111**, 2357 (1999).
[19] R. Kubo, N. Toda, and N. Hashitsume, *Statistical Physics II* (Springer, New York, 1985).
[20] B. J. Berne, in *Physical Chemistry: An Advanced Treatise,* edited by H. Eyring (Academic, New York, 1971), Vol. VIIIB, Chap. 9, p. 539.
[21] M. Pavese and G. A. Voth, Chem. Phys. Lett. **249**, 231 (1996).
[22] M. E. Tuckerman and B. J. Berne, J. Chem. Phys. **99**, 2796 (1983).
[23] A. S. Umar, J. Wu, M. R. Strayer, and C. Bottcher, J. Comput. Phys. **93**, 426 (1991).
[24] S. Jang and G. A. Voth, J. Chem. Phys. **111**, 2371 (1999).
[25] R. Ramirez, T. Lopez-Ciudad, and J. C. Noya, Phys. Rev. Lett. **81**, 3303 (1998).
[26] R. Ramirez and T. Lopez-Ciudad, J. Chem. Phys. **111**, 3339 (1999).
[27] M. R. Wall and D. Neuhauser, J. Chem. Phys. **102**, 8011 (1995).
[28] E. Rabani, B. Hetenyi, and B. J. Berne, J. Chem. Phys. **110**, 5238 (1999).